International Journal on Interactive Design and Manufacturing (IJIDeM)
https://doi.org/10.1007/s12008-023-01507-1

ORIGINAL PAPER

Neck orthosis design for 3D printing with user enhanced comfort features

Rita Ambu[1] · Salvatore Massimo Oliveri[2] · Michele Calì[2]

Received: 14 April 2023 / Accepted: 10 August 2023

Abstract
An area of interest in orthopaedics is the development of efficient customized neck orthoses, considered that pathologies which affect the neck area are widespread. Advanced acquisition and modelling approaches combined with Additive Manufacturing (AM) can potentially provide customized orthoses with improved performance and complexity. However, in the design of these devices, besides functional and structural requirements, benefit and comfort of the patient should be a main concern, in particular, at the early stage of design during the acquisition of the body's part, and while using the printed orthosis. In this paper, a scanning system with three sensors was developed which allows a fast, about 5 s, and accurate acquisition of the neck area with minimum discomfort for the patient. A neck orthosis with a ventilation pattern obtained by Topology Optimization (TO), lightened by about 35%, was also established. In fact, a main role for comfort is played by the ventilation pattern which contributes both to lightness and breathability. Its structural and comfort performance was evaluated in comparison with an orthosis with a ventilation pattern configured by Voronoi cells. Structural assessment was carried out by means of finite element analysis under main loading conditions. An evaluation of neck temperatures in relation to wearing 3D printed prototypes, manufactured with Hemp Bio-Plastic® filament, was finally conducted by means of a thermal imaging camera. TO orthosis prototype showed a better performance regarding thermal comfort, with a maximum increase of neck temperature less than 1 °C, which makes the proposed configuration very promising for user's comfort.

Keywords Orthosis modelling · Reverse engineering · CAD · Additive manufacturing · Topology optimization · Thermal comfort

1 Introduction

The role of Additive manufacturing (AM) for applications in the biomedical field has grown over the years since this technology can be beneficial for different purposes [1, 2]. These include the possibility of creating tissues and organoids, surgical tools, patient specific surgical models for preoperative planning and custom made prosthetics [3–7].

✉ Rita Ambu
rita.ambu@unica.it

Salvatore Massimo Oliveri
moliveri@dii.unict.it

Michele Calì
michele.cali@unict.it

[1] Department of Mechanical, Chemical and Materials Engineering, University of Cagliari, 09123 Cagliari, Italy

[2] Electric, Electronics and Computer Engineering Department, University of Catania, 95125 Catania, Italy

In orthopaedics, the design for AM of customized external devices has attracted researchers considered that these can be more advantageous with respect to prefabricated orthoses obtained with other techniques. In fact, AM custom-made orthoses have a better fit to the patient's body, contributing both clinically and as regards comfort to the benefit of the final user. Orthoses are generally categorized depending on the body's affected part. The applications reported in literature are mainly focused on the design of upper limbs orthoses [8–10]. Lower limbs orthoses, in particular, ankle—foot orthoses (AFOs), have also been considered [11–13]. Research findings have shown the possibility to successfully design functional devices and the capability of adapting the procedures for the use by the medical personnel.

The design for AM of customized cervical orthoses is an area of application less explored with respect to the above-mentioned applications. Few patient-based case studies [14, 15] were investigated or particular aspects relative to comfort [16, 17] were considered. Different design approaches

Published online: 12 September 2023

were proposed. In [14] the geometry of the orthosis was obtained by positioning a simple guide geometry, specifically, a cylinder, over the three-dimensional scan of the neck and deformation energy was used to generate a ventilated model. Deformation energy was obtained through Finite Element analysis, and by varying the coefficients of an algorithm for reaction diffusion, which is used to simulate a variety of patterns in nature, a mesh with variable strength and porosity could be achieved. By applying this method, various tentative prototypes were manufactured until the final design that best met functional and comfort requirements.

Methods for improving comfort with ventilation patterns were also proposed, as in [16], where an algorithm for generating ventilated casts depending on the temperature distribution of the body in the area of the orthosis, was described. The study also included an example of application to a neck orthosis.

Cervical orthoses are designed for neck motion restriction and are mostly used to support weak or painful neck muscles, to immobilize the neck following surgery or trauma, and to correct the cervical spine. Usually, three typologies of orthoses are available on the market, specifically, the lightest soft cervical collars for minor neck injuries, generally made of foam rubber coated with a soft pad, the widespread semi-rigid orthoses, and the most complex cervical thoracic orthoses which have also an extension support to protect the thoracic spine.

The use of these devices can cause discomfort which is influenced by the design and duration of wear, while being the design the most significant factor [18]. Furthermore, other drawbacks were also reported such as lack of hygiene, muscle atrophy, pain and skin rush [19].

A customized neck orthosis obtained with AM should potentially alleviate these problems by the adoption of a proper geometry, decrease in weight and improved breathability, and all of this contributes to the increase of comfort, being, at the same time, met the clinical requirements.

The procedure of design generally comprises the digital acquisition of the body's part, followed by the CAD modelling of the geometry based on the anatomical data and the introduction of a ventilation pattern. Finally, the geometry of the orthosis, optimized in terms of clinical and structural requirements, is 3D printed with a material properly chosen.

In this paper, the design of a neck orthosis for AM is reported with particular attention to the aspects of the procedure of design which directly involve the final user.

As previously mentioned, the first step of the procedure consists in the acquisition and digital reconstruction of the neck's geometry. Actually, there are not standardized procedures for morphology acquisition but the method used should be accurate and fast in order to reduce the time of acquisition during which the patient has to stand still.

Different methods can be used for the acquisition of subject's anatomy and, depending on the method used, data are expressed as point cloud, voxels or three dimensional coordinates of different anatomical points [20].

A reconstruction of the neck geometry can be obtained by means of Computed tomography (CT) which is a technique usually used for diagnostics and surgical planning. The digital representation of the outer surface of the neck can be recovered with good accuracy, as shown in [21], and used to model the orthosis. This is a methodology to be considered if CT scans of the patient are already available as part of the diagnostics. In fact, a main drawback of the method is that the subject, during scanning, is exposed to radiation which depends on its duration. In addition, the reconstruction of the outer surface of the neck requires a certain number of steps and can be time consuming. A different approach consists in the use of laser scanners and structured light scanners or low-cost devices with various arrangements for acquisition [14, 22, 23].

In this study, a scanning system with low-cost devices, specifically, three Kinect sensors RGB-depth cameras by Microsoft, was developed with a layout which allows an acquisition fast and accurate, with a limited discomfort for the patient and suitable for hospital setting.

As for the modelling, an important aspect which has direct impact on the final comfort is the geometrical configuration of the ventilation pattern, since it contributes both to weight reduction and to the breathability of the orthosis. Different methods can be used to obtain a ventilation pattern consistent with the mechanical stiffness and clinical requirements. The basic approach for generating openings consists in the introduction of a regular or random repetition of a basic feature. A more complex methodology involves the generation of an irregular pattern on the surface, typically a hollowed Voronoi Tessellation, which can be implemented in parametric CAD environment [24] or with ad hoc algorithms [16]. Finally, a hollowed configuration of the geometry of the orthosis can be obtained by applying a known method for design, such as Topology Optimization (TO).

These methodologies are discussed and, in particular, an application of Topology Optimization method for generating a ventilated neck orthosis is reported. TO is a design method generally used for obtaining a weight reduction in industrial components, by optimizing material distribution depending on loads and boundary conditions. This approach is mainly applied in automotive and aeronautical fields but applications of this methodology to prostheses [25, 26] and orthoses [15, 27] are also reported in literature. The model obtained was assessed by means of Finite Element (FE) analysis for different loading configurations and the results in terms of structural performance were compared with those of a neck othosis with a similar weight but having a ventilation pattern based on Voronoi cells.

The manufacturing of the models was made by means of a Fusion Deposition Modelling (FDM) 3D printer. A sustainable composite filament composed by polylactic acid (PLA) and hemp shives, patented as Hemp Bio-Plastic® (HBP) [28] was used. The material has improved stiffness in comparison with other most commonly used plastics for AM [29] and superficial finish in addition to the antibacterial properties of hemp [30], which can contribute to comfort. A thermal analysis on neck temperature distribution resulting from wearing the two 3D printed orthoses for a period of time was finally carried out for a qualitative evaluation of thermal comfort. Measurements of neck temperature in relation to the manufactured prototypes has highlighted that the geometry obtained by means of TO has an improved thermal comfort with respect to an orthosis with a ventilation pattern based on Voronoi cells with analogous weight reduction with respect to the full geometry.

The study was conducted on a voluntary subject from which a written informed consent to participate in the tests was obtained.

2 Materials and methods

2.1 Neck's geometry acquisition and reconstruction

The accurate real-time patient's neck anatomy acquisition is here considered as a main challenge for developing a practical procedure that can be easily reproduced and implemented in clinical setting for the creation of a neck orthosis. 3D acquisition of body surfaces with mobile sensors around the patient's body in protracted periods of time, which is often carried out, causes acquisition errors and artifacts since it can be very difficult to maintain fixed the patient's anatomy. This problem is particularly felt for children who are harder to hold perfectly still also for short periods of time.

Microsoft Azure Kinect DK ver. 3 devices (Fig. 1a), used in this study, can be considered among the best performing available depth sensors [31–33] to obtain real-time patient's anatomy acquisition. They integrate a 12 MP RGB camera, 1 MP depth sensor and 2 IR emiters (for WFOV and NFOV acquisition).

Kinect DK device is equipped with smaller and more powerful sensors than a previous version (Microsoft Kinect ver. 2) used by the authors in another research [34]. The device used has a 1-megapixel depth sensor (ToF HoloLens 2), a 12 megapixel RGB camera and two infra-red illuminators (IR emitters) which allow to obtain mappings of the object's depth with high accuracy in a very short time. An illuminator used in narrow field-of-view (NFOV) mode is aligned with the depth camera case. The illuminator used in wide field-of-view (WFOV) mode is tilted an additional 1.3 degrees downward relative to the depth camera (Fig. 1b).

Azure Kinect DK depth camera transmits raw modulated IR images to the host PC and implements the Amplitude Modulated Continuous Wave (AMCW) Time-of-Flight (ToF) principle according to which the camera casts modulated lighting in the near-IR (NIR) spectrum on the scene. This camera, therefore, records an indirect measurement of the time it takes for light to move from the camera itself to the scene and vice versa. The measurements conducted are processed to generate a depth map characterized by a set of Z coordinate values for each pixel of the image and calculated in units of millimeters. Along with a depth map, it is also possible to get a so-called clean integration runtime reading where the value of each pixel is proportional to the amount of light returned by the scene. The resulting image is similar to a normal integration runtime image (Fig. 1c). Figure 1c shows a sample depth map (left) and a corresponding clean integration runtime image (right). Figure 1b shows the overlap areas between RGB and depth cameras at a distance of 500 mm with RGB camera set to 16:9 and 4:3 respectively.

The three Kinect DK devices were synchronized with each other in order to make the real-time patient's anatomy acquisition system efficient and easy to use in hospital environment.

A **series configuration (daisy configuration)** that allows synchronization of a master device with 2 subordinate devices was adopted [35]. A proper software compiled by the authors made possible to synchronize the activation times of the sensors after a preliminary calibration. Figure 2a shows the series configuration of the three Kinect devices used to acquire in real-time the neck surface; Fig. 2b shows a prototype of the acquisition set-up.

After an initial calibration test, the optimal range of use, systematic depth errors, precision tests and multi-view reconstruction tests were performed. In particular, it was verified that the best layout is the one in which the three sensors are arranged equidistant from each other (at 120°) along a circumference with a diameter of 1000 mm.

2.1.1 Calibration

Prior to proceeding with the acquisition of the patient's 3D neck anatomy, it was necessary to calibrate the position of each camera with respect to a global coordinate system. The data provided by the sensors can be represented in two different geometries: the geometry of the colour camera or the geometry of the infrared camera. The term geometry, related to the RGB or IR sensors of the Azure Kinect camera, refers to a set of sensor properties, including the coordinate system, its resolution, and all intrinsic transformations.

Using the libraries provided by Microsoft (Azure Kinect SDK libraries) for the management of data recorded by the cameras a software "kinfusion" was compiled by the authors.

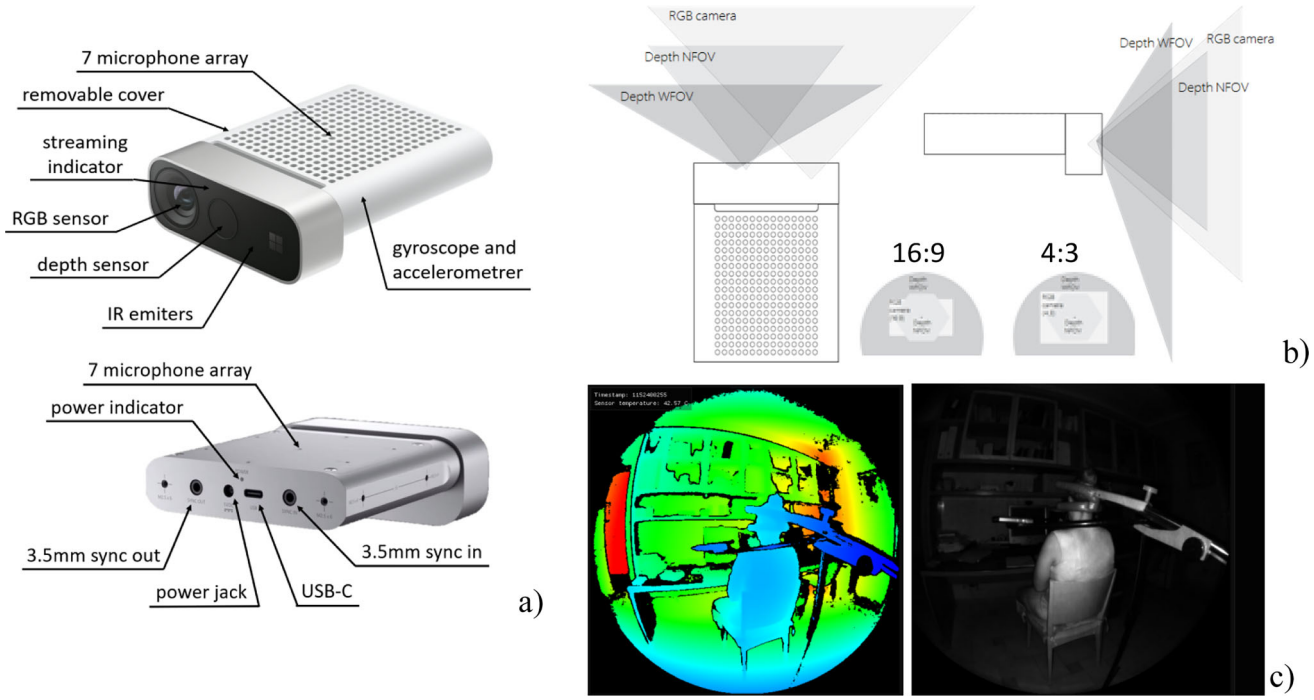

Fig. 1 **a** Sensors integrated in the Microsoft Azure Kinect DK device ver. 3, **b** Depth map and overlap areas between RGB and depth cameras, **c** Integration runtime image between RGB and depth cameras

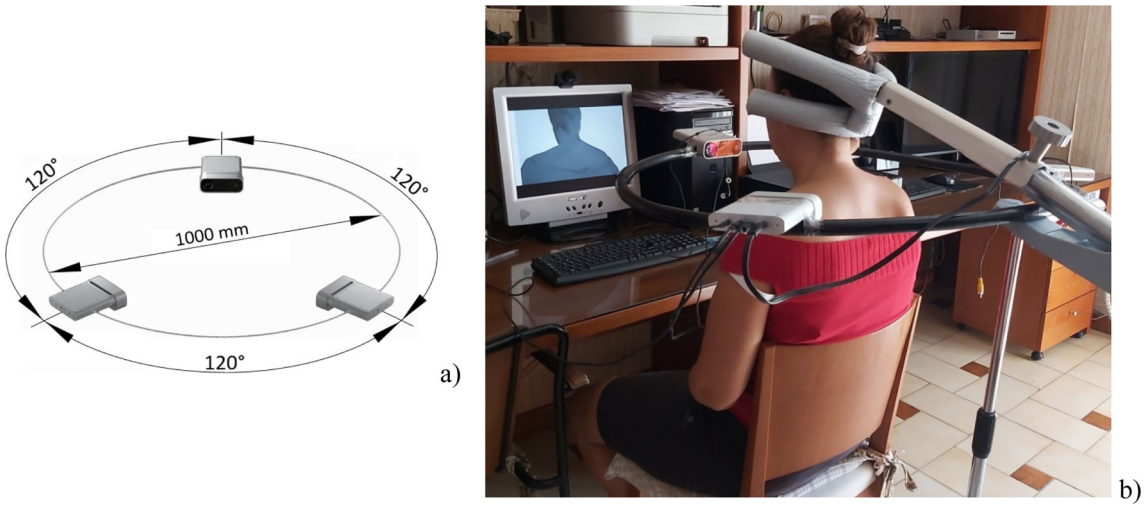

Fig. 2 **a** Series acquisition' layout of the three Kinect sensors, **b** Prototype of the acquisition set-up

2.1.2 Neck scan post-processing

The routines in the general SDK allow the integration of data from the three sensors to compose a single neck geometry. The integration takes place by overlapping semi-automatically, for an angular extension of just under 30 angular degree, the points and their depth maps provided by the three sensors. The overlap is realized using landmarks in correspondence with the most significant features of the parts to be joined. Figure 3 shows the landmarks used for the overlapping and the maximum errors measured in the overlap. It is possible to observe that in the zone of effective surfaces overlap the maximum error never exceeds the value of 1 mm (Fig. 3b).

The hardware located in the sensor allows the alignment of the acquisition time of colour and depth images. In practice, two types of synchronization were run at the same time: the **internal synchronization** that allows alignment between

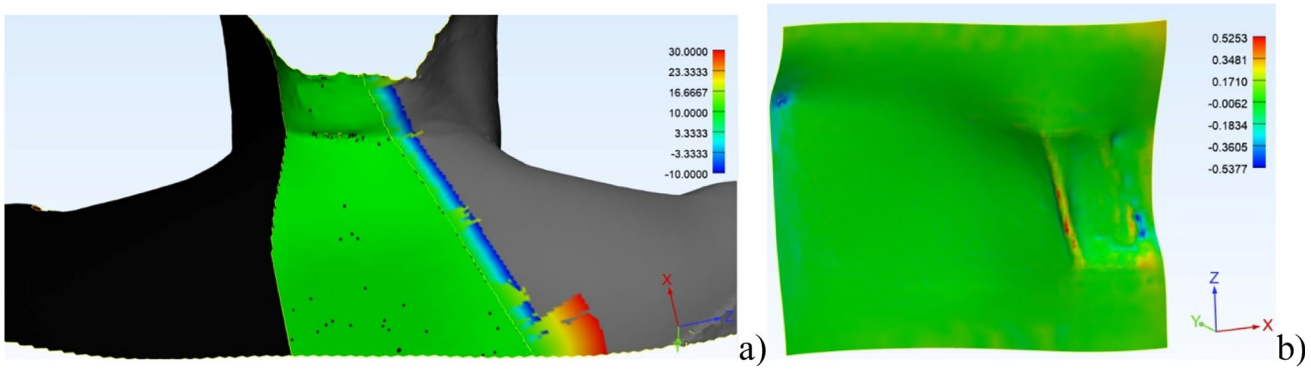

Fig. 3 Geometric overlap among acquisitions of three Kinect Microsoft sensors

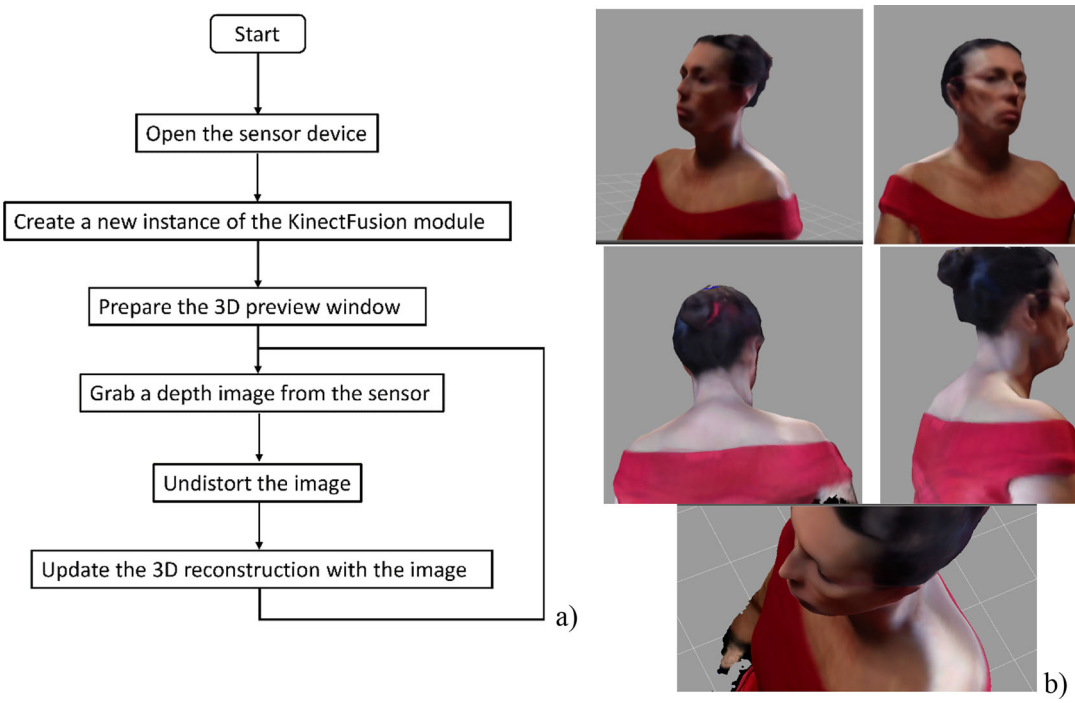

Fig. 4 Steps to obtain the points cloud

cameras in the same device and the **external synchronization** that allows the alignment of the acquisition time between multiple connected devices.

Using the CMake software, an internal synchronization was accomplished by preparing a "kinfusion" project in the Visual Studio 2017 environment and creating the OpenCV. In particular, the VTK was created by adding a new system environment variable. Once VTK and OpenCV were created, the kinfusion model was configured until its realization, as shown in the block diagram of Fig. 4.

Figure 5 shows the graphical interface (GUI) developed to manage "kinfusion" software.

The origin [0,0,0] is located at the focal point of the camera. The coordinate system is oriented such that the positive X-axis points right, the positive Y-axis points down, and the positive Z-axis points forward.

Figure 6 reports a final reconstruction of subject's anatomy including neck area.

2.2 Design of neck orthosis

The design of a neck orthosis essentially consists in the modelling of the geometry starting from the solid model of the neck and the introduction of a pattern of voids, or ventilation pattern, which should be compatible with functional and structural requirements.

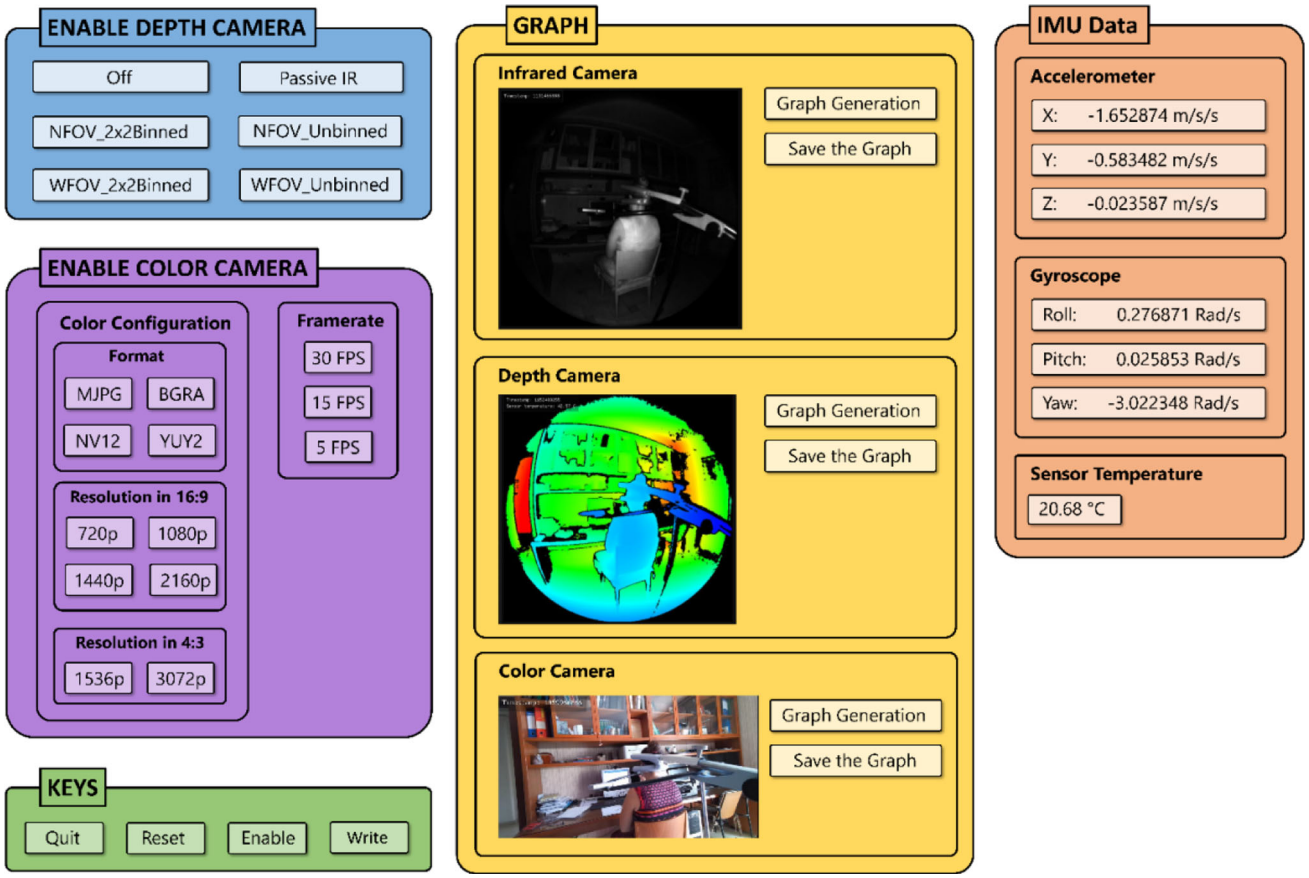

Fig. 5 GUI of "kinfusion" software

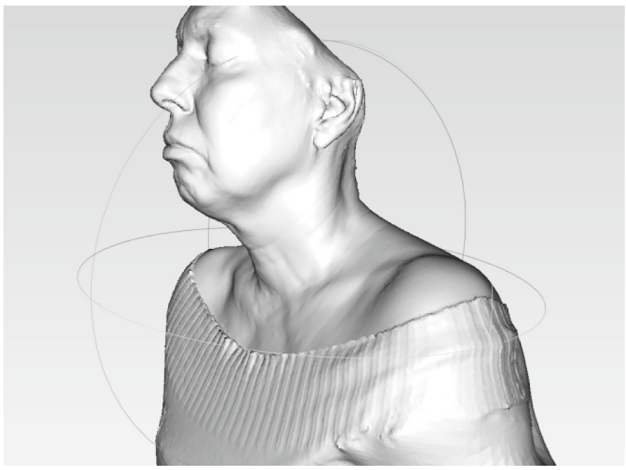

Fig. 6 Final reconstruction

2.2.1 Modelling of the geometry of the orthosis

The model of the neck is imported in CAD environment and, from that, a semi-automatic extraction of geometric reference features is performed in order to build the surface of the orthosis. The main steps of the procedure are reported in Fig. 7.

At first, a top plane is established by defining its position and orientation. At this aim, a central axis is created that goes about from the chin to the occipital bone (Fig. 7a). The choice of the axis should be guided by the medical personnel according to the morphology of the patient. The top plane is automatically defined with a local coordinate system and from there, downwards, the geometry of the model is built. In particular, further planes are created with a constant distance, except for areas where sudden changes in the silhouette occur, which require more planes for improved accuracy, until reaching the lower plane to be placed from the top of the chest to the back. In correspondence with these cut planes, the profiles resulting by the intersection of each plane with the neck geometry are automatically extracted (Fig. 7b). Once the profiles have been selected, a reference surface is obtained through these profiles by means of a loft operation (Fig. 7c). The surface is thickened and tailored, in particular, in the area of the chest and the shoulders, to the needs of a particular patient up to obtaining the final geometry, as shown in Fig. 7d. The model reported in the figure has a thickness of 4 mm.

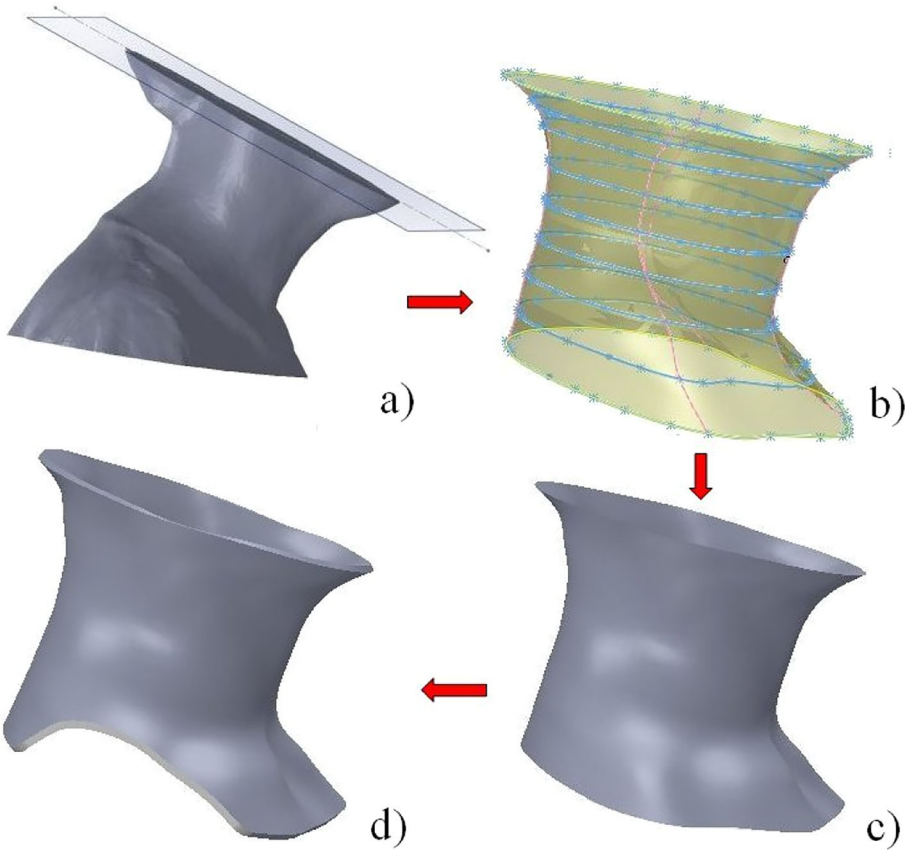

Fig. 7 Main steps of modelling

2.2.2 Ventilation pattern

A final goal in the design of an orthosis for AM is achieving a light structure satisfying at the same time the structural requirements. Generally, this is accomplished by the introduction of a pattern of voids, preferably with an automatic or semi-automatic technique, which is also useful for improving the breathability of the orthosis, thus reducing the risk of irritation. A ventilation pattern can be obtained in different ways and should be arranged also keeping areas devoid of the pattern, necessary for functional purposes and for inserting hinges and closures. Furthermore, the final configuration should be consistent with the loads exerted by the neck also in relation with the individual patient and the material chosen for manufacturing.

The simpler strategy consists in considering a geometric feature, such as a hole or similar, which is evenly or randomly repeated on the surface of the orthosis as shown in [21] where it was assessed that structural requirements can be satisfied with different geometrical patterns. However, this method has some drawbacks since it does not allow to optimize the distribution of the voids on the surface to obtain the lightest structures in relation to the capability of AM.

Another method for obtaining a ventilation pattern consists in establishing a pattern which is then mapped on the surface of the model. The final arrangement of the ventilation pattern on the orthosis depends on the geometry of the surface. This approach was considered by developing in Rhino-Grassoppher environment a procedure to map on the surface of the neck orthosis a hollowed Voronoi tessellation [34]. The workflow was configured providing the possibility to vary the areas to be excluded by the application of the ventilation pattern, for functional and design purposes. In fact, upper end areas of the orthosis in contact with the head should be preserved, as well as those located at the lower ends in contact with chest and shoulders. Furthermore, considered that the final orthosis is made with two halves, lateral areas devoid of the ventilation pattern should be provided for inserting hinges and closures. Geometrical configuration of the ventilation pattern on the surface can be easily varied by changing the parameters in order to obtain a personalized distribution of voids for a particular patient. Figure 8 shows an example of application of the procedure to the model reported in Fig. 7d.

It should be noted that the introduction of the ventilation pattern in the model reported in Fig. 8 allowed a weight reduction of about 35% with respect to the full model.

Both methods described for the generation of a ventilation pattern require a subsequent structural assessment to verify that, depending on the material chosen for manufacturing,

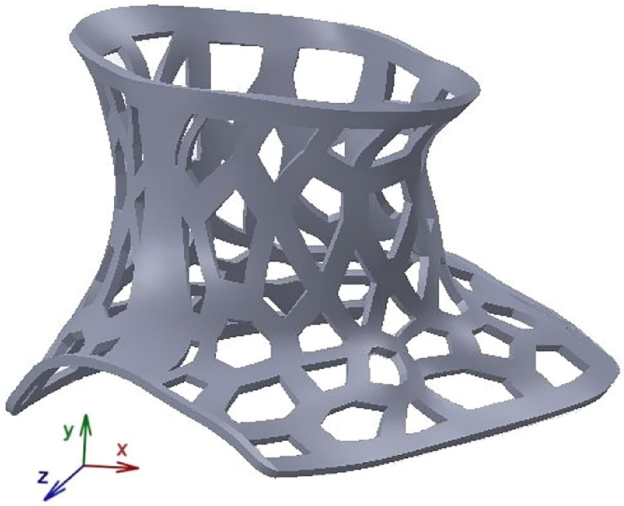

Fig. 8 Model of neck orthosis with Voronoi ventilation pattern

the orthosis can restrict neck motions withstanding forces exerted by the neck.

Another approach for obtaining a ventilation pattern is based on the application of Topology Optimization (TO) methodology that, as known, allows to obtain a lightened geometry of a part by the optimization of the material's distribution depending on loads and constraints acting on the part. This method was applied to the model of the orthosis reported in Fig. 7d, analogous, for comparison purposes, to the geometry used to obtain the Voronoi neck orthosis.

The material Hemp Bio-Plastic® (HBP), previously introduced, was used for simulations. The mechanical properties are: E = 4420 MPa and $\nu = 0.32$. TO methodology also requires to define constraints and objective. The defined objective was the minimization of the compliance of the model under a given amount of mass removal.

Loads exerted by the neck and constraint were then defined and applied to the model of the orthosis. The definition of the loads requires particular attention considered that the cervical spine and muscles of the neck are a complex structure. However, generally, the movements of the human neck taken into account to evaluate neck forces are essentially extension, flexion, lateral bending and axial rotation, since all other movements can be considered as a combinations of these loads.

Measurement of loadings of the cervical spine in vivo is complex and there is a large variation of data from literature. Modelling approaches were also proposed as in [36] where a methodology to generate models with detailed neck musculoskeletal architecture interactively scalable for anthropometry and muscle strength was reported.

Neck forces applied to the full model for applying TO procedure, were derived from an experimental study [37] where the three-dimensional maximum moments measured during maximum voluntary contractions of neck muscles were measured. The three most relevant movements, namely, extension, flexion and lateral bending were considered to derive forces that were applied at the upper end on the inside of the model. Extension force ($F_e = 287$N) and flexion force ($F_f = 165$N) act on the sagittal plane in opposite directions, while lateral bending force ($F_b = 208$N) originates a moment in the coronal or frontal plane. Control of symmetry was applied with respect to the sagittal plane in order to simulate the effect of lateral bending force on both sides. Finally, the model was fully constrained at the lower end. Figure 9a schematically shows loads and constraints applied to the model. The forces were derived by considering the highest values of the measured moments for women, expressed in the reference study in terms of media and standard deviation, keeping into account the characteristics of the subject for which the orthosis is intended. The distance between C7-T1 and the upper ends was approximately evaluated in order to obtain the lever arm as 0,115 m. The application of the procedure, carried out with the software nTopology (nTopology, Inc.), allowed to obtain a rough geometry, which was smoothed and used to redesign the final model which is reported in Fig. 9b.

The model reported in Fig. 9b satisfies the functional requirements relative to the preservation of the edge areas in the upper part of the orthosis as well as those necessary to insert hinges and closures. This model allowed a reduction of the weight of about 35% with respect to the full geometry.

3 Results and discussion

3.1 Numerical assessment of neck orthoses

TO model obtained was assessed with FE analysis to verify the validity of the final geometry. The model was meshed with tetrahedral elements and the simulations were carried out by applying loads and constraints as described in the previous paragraph. The first parameter considered in the analysis was the total displacement.

Figure 10 reports the iso-colour representation of total displacement, expressed in mm, relative to the different loading conditions considered.

The maximum value of the total displacement was obtained for extension loading, and the value obtained was under 2 mm, which can be considered relatively small.

The other parameter analyzed was Von Mises stress distribution. Figure 11 reports the iso-colour representations of Von Mises stress, expressed in MPa.

From the analysis it was highlighted that the maximum stress is obtained for extension loading and is acceptable considered that the value of the flexural maximum strength of HPB is 69.7 MPa.

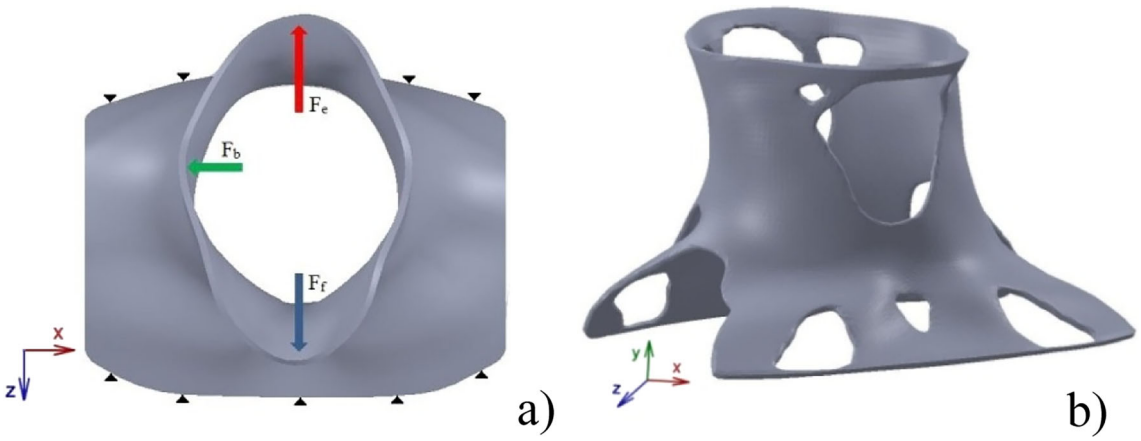

Fig. 9 Topology Optimization: **a** loads and constraints, **b** final model

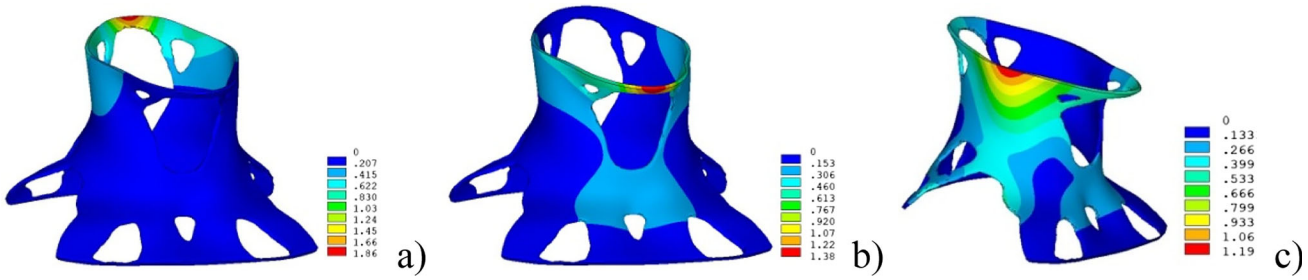

Fig. 10 Iso-colour representation of the total displacement for different loading: **a** extension, **b** flexion, **c** lateral bending

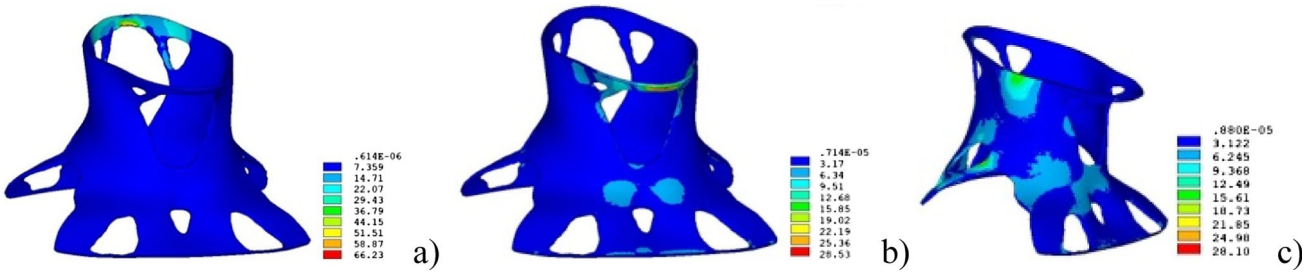

Fig. 11 Iso-colour representation of Von Mises stress distribution for different loading: **a** extension, **b** flexion, **c** lateral bending

These results can be evaluated in comparison with those of a similar analysis on the neck orthosis reported in Fig. 8, characterized by a ventilation pattern obtained by the application on the surface of a Voronoi tessellation. The two orthoses were obtained starting from the same full model and are characterized by a similar weight reduction. Analogous FE simulations were carried out and the same parameters were considered.

The diagrams in Fig. 12 report respectively the total displacement (a) and Von Mises stress (b) relative to the two different models considered for the three loading conditions.

The diagrams show a slightly higher values in correspondence of extension and flexion loadings for the model obtained with TO procedure. As for lateral bending, differently from the other loading conditions, higher values were obtained for the Voronoi model. However, for this loading condition, it should be noted that the values can be influenced by the different extension of the full area placed at the side and designed to allow the insertion of hinges and closures of the orthosis.

3.2 Additive manufacturing of prototypes

The final model of TO orthosis was done in two halves, as highlighted in Fig. 13, which are held together by means of lateral adjustable closures in order to assure the optimal fit of the device.

The sealing system of the two halves was designed with an adjustable fastening coupling, visible in the detail of Fig. 13. This allows to avoid misalignments of the two halves and

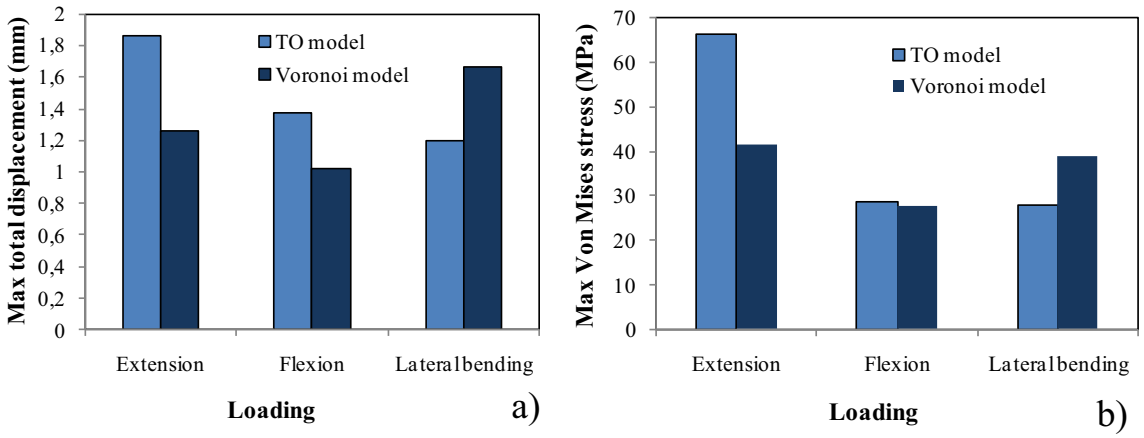

Fig. 12 Comparison between maximum displacement (**a**) and maximum Von Mises stress (**b**) for orthoses with different ventilation patterns

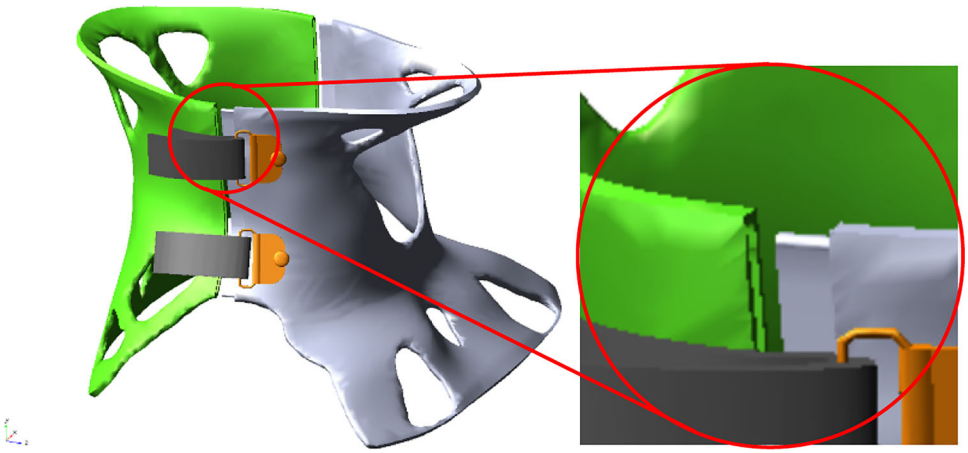

Fig. 13 Final design of TO neck orthosis

to regulate the adhesion to the neck even in the presence of a padding that should be inserted between the neck and the orthosis for improved comfort.

The orthosis was manufactured with a D300 Technology® 3D Printer which uses Fusion Deposition Modeling (FDM) methodology. The printer, equipped with a 0.6 mm nozzle, has an accuracy of 0.05 mm in the plane containing the printing bed and 0.1 mm in the vertical direction perpendicular to the print bed. The material used for printing was HPB, described in the introduction, whose characteristics, such as good superficial finish and antibacterial properties, can be advantageous also for comfort purposes. In addition, the material has the appearance of natural wood which also satisfies aesthetics. Figure 14 reports the manufactured prototype of the orthosis.

The two halves of the orthosis reported in the figure are linked with tentative adjustable closures which accomplish the functional requirements but still need to be improved as aesthetics.

Figure 15 reports the prototype of Voronoi neck orthosis manufactured with HPB.

3.3 Thermal verification of prototypes

TO orthosis was qualitatively evaluated in terms of thermal comfort, by means of measurements of neck temperature, in comparison with the model ventilated with the Voronoi tessellation. This is a limited analysis aimed at assessing the prototypes manufactured with HPB. The measurements on the neck area were made by using the thermal Imaging Camera HT-02 Dongguan Xintai Instrument Co. Ltd. The tests were performed with an ambient temperature of 17.8 °C and humidity 50%. Thermal images of the neck area were taken before and after wearing the orthoses for 30 min. In the analysis carried out the result of the insertion of a padding between the neck and the orthosis was also considered. The temperature distributions of the skin are reported in Fig. 16.

In particular, Fig. 16a shows the thermal map of the neck before wearing the orthosis. In Fig. 16b, c, the thermal maps of the neck after wearing TO orthosis, respectively without and with padding, are reported. The thermal maps of the neck after wearing the Voronoi orthosis without and with padding are reported respectively in Fig. 16d, e.

Fig. 14 Printed prototype of TO neck orthosis

Fig. 15 Printed prototype of Voronoi neck orthosis

Thermal maps share the same colour scale and besides the temperature value measured at a point taken as a reference just above the orthoses and near the ear is highlighted (value shown at the top left).

Thermal maps show how the TO orthosis allows a good ventilation of the neck. The maximum temperature on the neck after wearing the orthosis for 30 min increases by only 0.7 °C (Fig. 16b). The area affected by this increase is quite limited and the temperature in the areas close to the orthosis undergoes a temperature rise of only a few tenths of a degree. Also with the use of a padding on this type of orthosis, the geometry configuration allows to limit the temperature increases on the neck (Fig. 16c).

After wearing TO orthosis with the padding for 30 min, the area subjected to temperature increase is quite limited and the temperature in the areas close to the orthosis undergoes an increase of only a couple of tenths of a degree. Therefore, even using padding the TO orthosis continues to guarantee a good ventilation.

The same analysis performed on the Voronoi orthosis showed that the insertion of the padding determines a slight increase in temperature, as expected. The comparison between the thermal map of the neck surface obtained after wearing the Voronoi orthosis (Fig. 16d) and that corresponding to the TO orthosis shows a better thermal comfort for the latter. This is evident by also considering the lower temperatures measured in the upper part of the head.

The difference between the two types of orthoses is then even more evident considering that, after wearing the Voronoi orthosis with a padding for 30 min (Fig. 16e), a maximum temperature of 38.3° C is registered as well as an overall increase of one degree in the neck areas taken as a reference for the comparisons made.

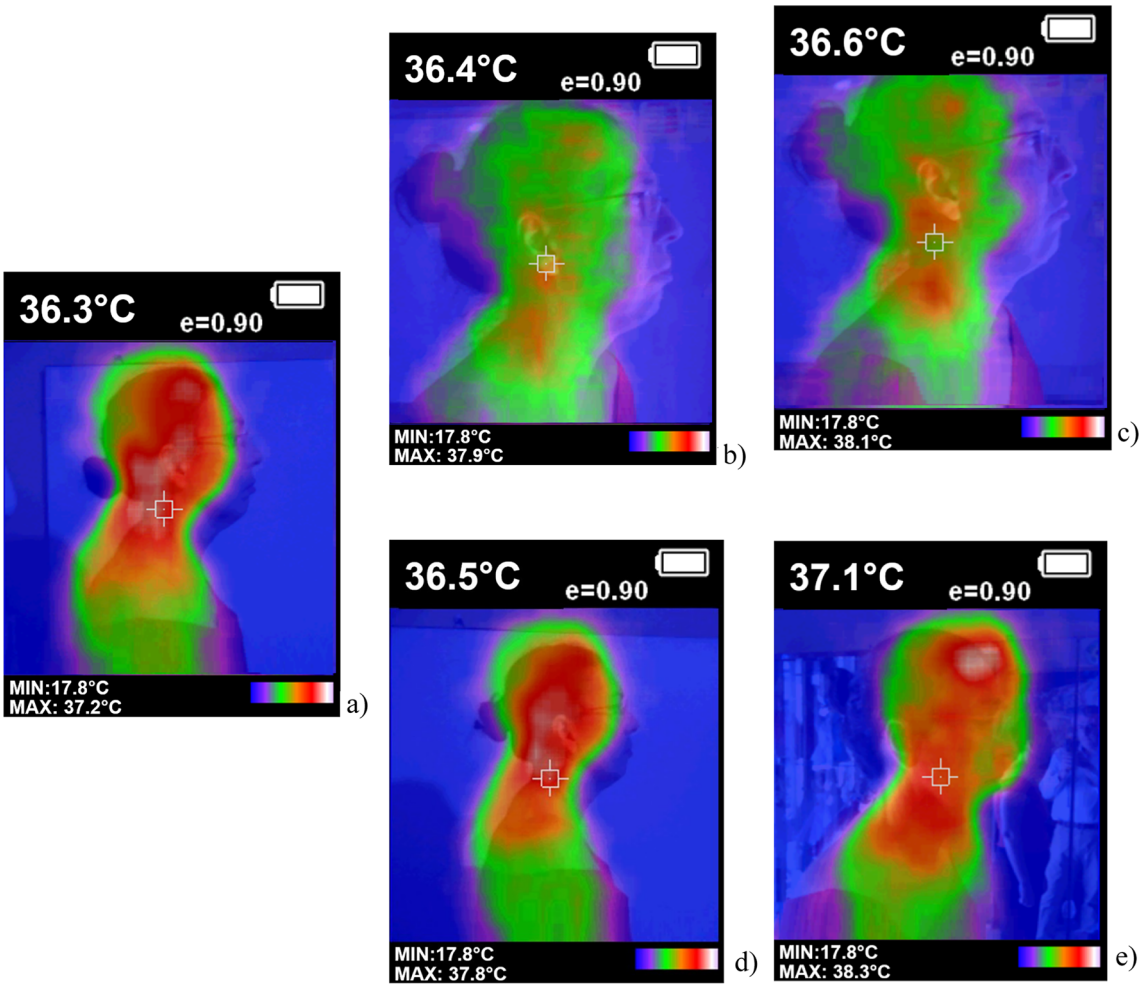

Fig. 16 Maps of temperature distribution: **a** neck before wearing orthosis, **b** after 30 min wearing TO orthosis without padding, **c** after 30 min wearing TO orthosis with padding, **d** after 30 min wearing Voronoi orthosis without padding; **e** after 30 min wearing Voronoi orthosis with padding

4 Conclusions

In this paper an overall procedure for the design of a neck orthosis for AM is reported and some issues aimed at improving comfort for the patient are considered.

A scanning system made up of three synchronized low cost sensors, suitably arranged, has been developed. This system allows a fast acquisition, about 5 s, with minimum discomfort for the patient. The scanning system is also potentially suitable to hospital setting, being low cost and provided with a GUI for semi-automatic management of the device. Efficiency in the acquisitions should be also potentially increased by the use of statistical shape models of the neck which could be obtained by means of methodologies, such as mesh morphing, as reported in [38] for other body parts.

Regarding modelling, different configurations of the ventilation pattern, which mostly contribute to weight reduction and comfort of the orthosis, are discussed and a new topology optimized configuration is proposed.

TO model, structurally evaluated by means of FE analysis, also in comparison with an orthosis having a ventilation pattern configured as Voronoi cells, showed a satisfactory behaviour also considered that, voids are large and, in particular for extension and flexion loading, stress distribution occurs in areas of limited size with reference to the extent of the upper parts where the load is applied. The highest values of maximum displacement and maximum Von Mises stress were obtained for extension loading; however, maximum displacement was lower than 2 mm, while maximum stress was under the limit value for HPB.

The manufacturing of prototypes was done with a new bio-based material, which also contribute to lightness and satisfies the aesthetic demands. Neck temperature measurements, made in relation with the use of the two different orthoses, highlighted a better performance for the TO orthosis even with the insertion of a padding. The maximum increase of temperature after wearing the prototype for

30 min was lower than 1 °C, assessing a reasonable ventilation of the neck. These tests were mainly aimed at assessing the manufactured prototypes and performance of the advanced material HPB. However, thermal measurements in relation to wearing the proposed orthosis are promising and further extended tests on thermal comfort and, more generally on user's satisfaction also with the use of questionnaire are necessary and foreseen in future research.

As for the methodology for obtaining ventilation patterns, more effort is necessary for developing a procedure where a predetermined TO pattern might be easily adapted to the individual patient, while mapping on the surface of the orthosis of patterns based on Voronoi cells, being developed in Visual Language, is more adaptable for the use by non CAD-experts. However, considered that TO orthosis is very promising as regards user's comfort, an automatized strategy for the procedure will be investigated.

Funding Open access funding provided by Università degli Studi di Cagliari within the CRUI-CARE Agreement. The fund was provided by Università di Catania (PIACERI 2020/22-GOSPEL/UPB:61722102132).

Declarations

Conflict of interest The authors declare that they have no conflict of interest to report.

Ethics approval and consent to participate In light of the Declaration of Helsinki, patient gave oral informed consent to start the intervention. In addition, a written informed consent to participate in the tests was obtained.

Consent for publication All authors give consent to the publication of this manuscript. Written consent for publication was obtained from the patient whose photographs have been used in this study.

References

1. Francis, M.P., Kemper, N., Maghdouri-White, Y., Thayer, N.: Additive manufacturing for biofabricated medical device applications. In: Zhang, J., Jung, Y.G. (eds.) Additive Manufacturing, Materials, Processes, Quantifications and Applications, pp. 311–344. Elsevier, Oxford (2018)
2. Khamkar, P., et al.: In: Banga, H.K., Kumar, R., Kalra, P., Belokar, R.M. (eds.) Additive Manufacturing with Medical Applications. CRC Press, Berlin (2022)
3. Ganguli, A., Pagan-Diaz, G.J., Grant, L., Cvetkovic, C., Bramlet, M., Vozenilek, J., Kesavadas, T., Bashir, R.: 3D printing for preoperative planning and surgical training: a review. Biom. Microdevices **20**, 65 (2018). https://doi.org/10.1007/s10544-018-0301-9
4. Wong, K.C., Kumta, S.M., Sze, K.Y., Wong, C.M.: Use of a patient specific CAD/CAM surgical jig in extremity bone tumor resection and custom prosthetic reconstruction. Comput. Aided Surg. **17**(6), 284–293 (2012)
5. Guachi, R., Bici, M., Bini, F., Calispa, M.E., Oscullo, C., Guachi, L., Campana, F., Marinozzi, F.: 3D Printing of Prototypes Starting from Medical Imaging: A Liver Case Study. In: Rizzi, C., Campana, F., Bici, M., Gherardini, F., Ingrassia, T., Cicconi, P. (eds) Design Tools and Methods in Industrial Engineering II. ADM 2021. Lecture Notes in Mechanical Engineering. Springer, Cham (2022). https://doi.org/10.1007/978-3-030-91234-5_54
6. Wan, Y., Tan, Q., Pu, F., Boone, D., Zhang, M.: A review of the application of additive manufacturing in prosthetic and orthotic clinics from a biomechanical perspective. Engineering **6**(11), 1258–1266 (2020). https://doi.org/10.1016/j.eng.2020.07.019
7. Zanetti, E.M., Aldieri, A., Terzini, M., Calì, M., Franceschini, G., Bignardi, C.: Additively manufactured custom load-bearing implantable devices: grounds for caution. AMJ **10**(8), 694–700 (2017). https://doi.org/10.21767/AMJ.2017.3093
8. Paterson, A.M., Bibb, R., Campbell, R.I., Bingham, G.: Comparing additive manufacturing technologies for customised wrist splints. Rapid Prototyp. J. **21**(3), 230–243 (2015). https://doi.org/10.1108/RPJ-10-2013-0099
9. Buonamici, F., Furferi, R., Governi, L., Lazzeri, S., McGreevy, K.S., Servi, M., Talanti, E., Uccheddu, F., Volpe, Y.: A practical methodology for computer-aided design of custom 3D printable casts for wrist fractures. Vis. Comput. **36**, 375–390 (2020). https://doi.org/10.1007/s00371-018-01624-z
10. Baronio, G., Harran, S., Signoroni, A.: A critical analysis of a hand orthosis reverse engineering and 3d printing process. Appl. Bionics Biomech. (2016). https://doi.org/10.1155/2016/8347478
11. Wojciechowski, E., Chang, A.Y., Balassone, D., Ford, J., Cheng, T.L., Little, D., Menezes, M.P., Hogan, S., Burns, J.: Feasibility of designing, manufacturing and delivering 3D printed ankle-foot orthoses: a systematic review. J. Foot Ankle Res. **12**(11), 11 (2019). https://doi.org/10.1186/s13047-019-0321-6
12. Alqahtani, M.S., Al-Tamimi, A., Almeida, H., et al.: A review on the use of additive manufacturing to produce lower limb orthoses. Prog. Addit. Manuf. **5**, 85–94 (2020). https://doi.org/10.1007/s40964-019-00104-7
13. Banga, H.K., Kalra, P., Belokar, R.M., Kumar, R.: Customized design and additive manufacturing of kids' ankle foot orthosis. Rapid Prototyp. J. **26**(10), 1677–1685 (2020). https://doi.org/10.1108/RPJ-07-2019-0194
14. Hale, L., Linley, E., Kalaskar, D.M.: A digital workflow for design and fabrication of bespoke orthoses using 3D scanning and 3D printing, a patient-based case study. Sci. Rep. **10**, 7028 (2020). https://doi.org/10.1038/s41598-020-63937-1
15. Xu, Y., Li, X., Chang, Y., Wang, Y., Che, L., Shi, G., Niu, X., Wang, H., Li, X., He, Y., Pei, B., Wei, G.: Design of personalized cervical fixation orthosis based on 3D printing technology. Appl. Bionics. Biomech. **202**, 8243128 (2022). https://doi.org/10.1155/2022/8243128
16. Zhang, X., Fang, G., Dai, C., Verlinden, J., Wu, J. Whiting, E., Wang, C.C.L.: Thermal-comfort design of personalized casts. In: UIST 2012 Proceedings, pp.243–254, Quebec City, Canada (2017). https://doi.org/10.1145/3126594.3126600

17. Prates, A.: Self-adjusting orthoses design. Scripta-Ingenia **3**, 3–8 (2014)
18. Langley, J., Pancani, S., Kilner, K., Reed, H., Stanton, A., Heron, N., Judge, S., McCarthy, A., Baxter, S., Mazzà, C., McDermott, C.J.: A comfort assessment of existing cervical orthoses. Ergonomics **61**(2), 329–338 (2018). https://doi.org/10.1080/00140139.2017.1353137
19. Worsley, P.R., Stanger, N.D., Horrell, A.K., Bader, D.L.: Investigating the effects of cervical collar design and fit on the biomechanical and biomarker reaction at the skin. Med. Devices Evid. Res. **11**, 87–94 (2018). https://doi.org/10.2147/MDER.S149419
20. Barrios-Muriel, J., Romero-Sánchez, F., Alonso-Sánchez, F.J., Rodríguez Salgado, D.: Advances in orthotic and prosthetic manufacturing: a technology review. Materials (Basel) **13**(2), 295 (2020). https://doi.org/10.3390/ma13020295
21. Ambu, R., Motta, A., Calì, M. Design of a customized neck orthosis for FDM manufacturing with a new sustainable bio-composite. In: Rizzi, C., Andrisano, A.O., Leali, F., Gherardini, F., Pini, F., Vergnano, A. (eds) Design Tools and Methods in Industrial Engineering. ADM 2019. Lecture Notes in Mechanical Engineering. Springer, Cham (2020). https://doi.org/10.1007/978-3-030-31154-4_60
22. Rogati, G., Leardini, A., Ortolani, M., Caravaggi, P.: Validation of a novel Kinect-based device for 3D scanning of the foot plantar surface in weight-bearing. J Foot Ankle Res **12**, 46 (2019). https://doi.org/10.1186/s13047-019-0357-7
23. Xhimitiku, I., Pascoletti, G., Zanetti, E.M., Rossi, G.: 3D shape measurement techniques for human body reconstruction. Acta IMEKO **11**(2), 1–8 (2022). https://doi.org/10.21014/acta_imeko.v11i2.1119
24. Li, J., Tanaka, H.: Feasibility study applying a parametric model as the design generator for 3D–printed orthosis for fracture immobilization. 3D Print Med **4**, 1 (2018). https://doi.org/10.1186/s41205-017-0024-1
25. Jansari, T., Deiab, I.: Comparative study of a topologically optimized lower limb prosthesis. IJIDeM **13**, 645–657 (2019). https://doi.org/10.1007/s12008-019-00540-3
26. Iqbal, T., Wang, L., Li, D., Dong, E., Fan, H., Fu, J., Hu, C.: A general multi-objective topology optimization methodology developed for customized design of pelvic prostheses. Med Eng Phys **69**, 8–16 (2019). https://doi.org/10.1016/j.medengphy.2019.06.008
27. Zolfagharian, A., Gregory, T.M., Bodaghi, M., Gharaie, S., Fay, P.: Patient-specific 3D-printed splint for mallet finger injury. Int J Bioprint **6**(2), 259 (2020). https://doi.org/10.18063/ijb.v6i2.259
28. https://www.kanesis.it/products/#filaments, last accessed 2019/06/26.
29. Calì, M., Pascoletti, G., Gaeta, M., Milazzo, G., Ambu, R.: A new generation of bio-composite thermoplastic filaments for a more sustainable design of parts manufactured by FDM. Appl. Sci. **10**, 5852 (2020). https://doi.org/10.3390/app10175852
30. Khan, A.K., Warner, P., Wang, H.: Antibacterial properties of hemp and other natural fibre plants: a review. BioResources **9**(2), 1–18 (2014). https://doi.org/10.15376/biores.9.2.3642-3659
31. Clarkson, S., Wheat, J., Heller, B., Choppin, S.: Assessing the suitability of the microsoft kinect for calculating person specific body segment parameters. In: Agapito, L., Bronstein, M., Rother, C. (eds) Computer Vision - ECCV 2014 Workshops. ECCV 2014. Lecture Notes in Computer Science(), vol 8925. Springer, Cham (2015). https://doi.org/10.1007/978-3-319-16178-5_26
32. Carfagni, M., Furferi, R., Governi, L., Servi, M., Uccheddu, F., Volpe, Y., et al.: Fast and low-cost acquisition and reconstruction system for human hand-wrist-arm anatomy. Proced. Manuf. **11**, 1600–1608 (2017). https://doi.org/10.1016/J.PROMFG.2017.07.306
33. Carfagni, M., Furferi, R., Governi, L., Servi, M., Uccheddu, F., Volpe, Y.: On the performance of the intel SR300 depth camera: metrological and critical characterization. IEEE Sens. J. **17**, 4508–4519 (2017). https://doi.org/10.1109/JSEN.2017.2703829
34. Ambu, R., Oliveri, S.M., Calì, M.: A bespoke neck orthosis for additive manufacturing with improved design method and sustainable material. In: Rizzi, C., Campana, F., Bici, M., Gherardini, F., Ingrassia, T., Cicconi, P. (eds.) Design Tools and Methods in Industrial Engineering II. ADM 2021. Lecture Notes in Mechanical Engineering. Springer, Cham (2022). https://doi.org/10.1007/978-3-030-91234-5_5
35. Intel®RealSenseTM Technology: http://www.intel.com/content/www/us/en/architecture-and-technology/realsense-overview.html (2015). Accessed 4 May 2022
36. Roos, P.E., Vasavada, A., Zheng, L., Zhou, X.: Neck musculoskeletal model generation through anthropometric scaling. PLoS ONE **15**(1), e0219954 (2020). https://doi.org/10.1371/journal.pone.0219954
37. Vasavada, A.N., Li, S., Delp, S.L.: Three-dimensional isometric strength of neck muscles in human. Spine **26**(17), 1904–1909 (2001). https://doi.org/10.1097/00007632-200109010-00018
38. Pascoletti, G., Aldieri, A., Terzini, M., Bhattacharya, P., Calì, M., Zanetti, E.M.: Stochastic PCA-based bone models from inverse transform sampling: proof of concept for mandibles and proximal femurs. Appl. Sci. **11**, 5204 (2021). https://doi.org/10.3390/app11115204